

MODELLING OF CORROSION INHIBITION OF CUCUMBER PLANT EXTRACTS ON AISI 1007 STEEL IN SEA WATER

Yusuf Lanre SHUAIB-BABATA^{1*}, Hassan Kobe IBRAHIM²,
Yusuf Olarenwaju BUSARI¹, Rasheedat Modupe MAHAMOOD¹,
Sikiru Ottan ABDULRAMAN³, Ibrahim Owolabi AMBALI¹,
Babatunde Lawal ABDULQADIR⁴, Ishaq Na'allah AREMU¹,
Kabiru Sulaiman AJAO¹, Samuel Omojola EJIKO⁵

¹Department of Materials & Metallurgical Engineering, University of Ilorin, Nigeria

²Department of Mechanical Engineering, University of Ilorin, Ilorin, Nigeria

³Department of Mechanical Engineering, Kwara State University, Malete, Nigeria

⁴Department of Mechanical Engineering, Kwara State Polytechnic, Ilorin, Nigeria

⁵Department of Mechanical Engineering, Federal Polytechnic, Ado-Ekiti, Nigeria

e-mail: sylbabata@unilorin.edu.ng; sylbabata@gmail.com

ABSTRACT

Adsorption Models with the application of corrosion experimental data is a very popular mechanism to predict various inhibitive systems. The effective modelling and interpretation of adsorption isotherms reliably determine the level of accuracy of adsorption processes. This study aims to apply the adsorption models and inhibitive mechanism of Cucumber Peel Extract (CPE) and Cucumber Seed Oil (CSO) to corrosion of AISI 1007 steel grade in the saline medium using both the electrochemical (Tafel Polarisation) and non-electrochemical (Weight Loss) techniques. The chemical composition of AISI 1007 and the phytochemical properties of studied extracts were determined. Consideration was given to Langmuir and Dubinin-Radushkevich Isotherm models (D-RIM) to study the inhibitive properties of CPE and CSO on AISI 1007 steel in an aggressive medium. The result of inhibition efficiency from weight loss measurement showed maximum inhibitions of 94.44 % and 95.44 % with 1.0 g/L concentration of CPE and CSO respectively in sea water medium. The result of the studied extract at 25 °C in seawater showed that the corrosion current density of AISI 1007 steel decreased and increased in the inhibition efficiency with 87.33% and 94.67% for CPE and CSO respectively. The negative value of ΔG_{ads} was greater than 20 kJ/mol and was obtained as a result of electrostatic interaction between the adsorbed inhibitor molecules and the ions/atoms on the metal surface. The studied inhibitors were confirmed to be mixed organic corrosion inhibitors type. The values of E and maximum surface coverage (θ_{max}) for the two measurements are satisfactorily in acceptable agreement as similar to the range of value obtained for inhibition efficiency.

KEYWORDS: adsorption; mechanism; modelling; cucumber; corrosion

1. Introduction

The use of inhibitors is one of the superlative processes to improve corrosion resistance of metals caused by acid solutions such as in desalination plants as well as in other industrial applications. Recently, efforts have been shifted towards the formulation of safe inhibitors, like plant extracts that have become the reliable eco-friendly, readily available, and

renewable sources of effective corrosion inhibitors [1, 2]. The inhibition characteristics of green inhibitors exhibit varying inhibitive properties using different interpretations of adsorption isotherm models. Ayawei *et al.* provided an evaluation of all adsorption isotherm applications using both linear and non-linear regression analysis. In addition to error functions for optimal adsorption analysis and among the review models, the two-parameter isotherm has been

considered one of the most widely used tools for identifying the best-fitting adsorption models due to its estimation of the distribution of adsorbates throughout the surface coverage, evaluation of the adsorption system, and validation of the consistent quality of the theoretical assumptions of the adsorption isotherm model [3].

In recent time, Langmuir, Freundlich, Dubinin-Radushkevich, Temkin and Flory-Huggins models have been considered for green corrosion inhibition analysis among others [4]. Many researchers reported the use of these isotherm models for modelling of experimental data in predicting the inhibitive mechanisms of plant extracts such as Bitter Leaves Root, Watermelon Rind, Cucumis Sativus (Cucumber), Senecio anteuphorbium Leaves, and Acacia Tortilis Bark and Leaves [4-8]. However, the model used to investigate the mechanism of these green inhibitors on the surface of the metal is acidic media, and the feasibility of experimental techniques for corrosion is also required. Therefore, this study applied two different adsorption models to predict the viability of experimental techniques and the mechanism of corrosion inhibition on AISI 1007 Steel in natural seawater medium using Cucumber plant extract.

2. Methods and materials

2.1. Preparation of Inhibitors

The Cucumber (*Cucumis sativus*) was obtained locally in Ilorin, Nigeria. To remove unwanted material, the vegetable was thoroughly washed and peeled. The cucumber was cut for a proper view of the seed, and the seeds were carefully removed. The peel and seeds were air-dried at room temperature, and pulverized into 20 μ m. The weighed inhibitor was stored in desiccators prior to use. To prevent evaporation, a 20 g ground sample was combined with ethanol and sealed firmly for 48 hours. To obtain a high concentration of the produced extracts, the Cucumber peel Extract (CPE) and Cucumber Seed Oil (CSO) were filtered. The filtered solution was heated in a rotary evaporator for 20 minutes at 78 °C in a rotary evaporator configuration to expel the ethanol.

2.2. Preparation of Specimens

The 1.5 mm thickness of AISI 1007 steel specimens' elemental compositions was determined with spectrometer (Serial number: 15007384) containing 0.015% P, 0.008% S, 0.220% Mn, 0.033% C, 0.034% Si, 0.038% Cr, 0.007% Ni, 0.011% Al, 0.004% Co, 0.021% Cu. The corrosion specimens

were prepared according to ASTM G4 standard [9]. The coupon dimensions of 2.2 x 1.7 x 0.15 cm were polished to a mirror finish, degreased with trichloroethylene, and properly labeled for identification with rope, and for easy removal from the environment. Subsequently, the specimens were degreased in ethanol, air-dried in acetone, and stored in desiccators.

2.3. Weight Loss Method

The composition of the used seawater was carried out at the Chemistry Department laboratory, University of Ilorin, Ilorin, Nigeria, presented in Table 1. The preparing, cleaning, and evaluating Corrosion Test specimens were carried out according to ASTM G1 standard [10]. The specimens were weighed with an electronic weighing machine (HX 302T) with an accuracy of ± 0.01 g to establish the initial weight of the specimens (W1) and subsequent measurements.

Table 1. The composition of seawater

Composition	Value
pH Value	8.90
Electrical Conductivity	123.50
Turbidity (NTU)	10.42
Chloride ion (mg/l)	15.20
NaCl (mg/l)	63.7
Na ion (mg/l)	48.50

The immersion corrosion testing of specimens was conducted according to ASTM G31 standard [11]. The prepared steel specimens were immersed in 750 mL of seawater with and without varying concentrations of Cucumber extract (Peel and Seed oil). The concentrations of the cucumber extracts (peel and seed oil) were altered from 0.1 g/L to 1.0 g/L. All the test specimens were removed from the solutions every 24 hours for consecutive 3 days and 168 hours intervals for 1 month then the specimens were air-dried. The dried specimen was then reweighed to determine the difference in the weight of the specimens. The procedures were repeated for 24 hours intervals for the first 3 days and 168 hours intervals for 14, 21, and 28 days of exposure. From the weight loss, the Corrosion rate and Inhibiting efficiency (IE %) and surface coverage of the plant extracts were determined using Equation 1 [2]:

$$\text{Corrosion rate (mpy)} = \frac{534W}{DAT} \quad (1)$$

W is the change in weight of the specimen (g), D = 7.85 g/cm³, the specimen's constant density; A is the surface area of the AISI 1007 steel coupon (cm²),

while (T) is the exposure period in (hour). The percentage inhibiting efficiency (IE %) using the Equation 2 [4]:

$$I.E (\%) = \frac{CR_{Black} - CR_{inh}}{CR_{Black}} \times 100 \quad (2)$$

where: CR_{Black} = Corrosion rate in the absence of inhibitor, CR_{inh} = Corrosion in the presence of inhibitor.

2.4. Electrochemical Measurement

Electrochemical studies shown in Figure 1 were carried out at room temperature using a system with three electrode cells having AISI 1007 steel samples as working electrodes (having a 1.0 cm² exposed area), a saturated calomel electrode as the reference electrode, and a graphite rod as the auxiliary/counter electrode. The exposed area (1.0 cm²) of the working electrode (AISI 1007 Steel) was polished with a series of emery sheets of variable grades and washed thoroughly with double distilled water prior to immersion in the cell. During the polarization experiment, 0.01 V s⁻¹ was taken as the scan rate, 0.0 s hold time at E_f , and 2.0 s as quiet time. Potentiostat (VersaSTAT) was used as an electrochemical workstation. The workstation is embedded with software including DC105 for the TAFEL Polarisation. The experimental data was obtained for data analysis. The Tafel polarization curve showed the called Tafel behavior, which is the linear behavior in the E against log (i) plots. The E_{corr} and i_{corr} were determined by extrapolation of the slope in the polarization curves back to the corrosion potential.

The corrosion current density i_{corr} or corrosion rate is represented by the point of intersection, and the related potential at that point is E_{corr} . The corrosion rate (MPY) used for potentiodynamic polarization is given by Popov [12]:

$$CR (MPY) = \frac{0.131 \times I_{corr} \times EW}{d} \quad (3)$$

where $d = 7.874 \text{ kg/m}^3$ (iron metal's density), and EW is the equivalent weight per valence state of iron metal in oxidized form of 2 is 27.92.

The Inhibition efficiency (% IE.) of AISI steel samples was computed based on corrosion current density measurements of inhibited AISI steel electrode (i_{corr}) using the following relationship [8]:

$$IE (\%) = \frac{i_0 - i_a}{i_a} \times 100 \quad (4)$$

where i_a is the corrosion current for the control sample, and i_0 is the corrosion current for the inhibited samples at different concentrations.



Fig. 1. TAFEL Setup

2.5. Adsorption Models

The Langmuir isotherm model was considered to investigate the mechanism of the interaction between the inhibitor and the AISI 1007 steel surface. The effect of surface coverage (θ) was determined for different concentrations of the studied extracts (inhibitors) from weight loss and electrochemical measurements with expression $IE \% = \theta \times 100$ as reported by Awe *et al.* [4]. The equilibrium constant (K_{ads}) of the adsorption process was obtained from the isotherm model [8] as follows:

$$\frac{C}{\theta} = \frac{1}{K_{ads}} + C \quad (5)$$

where C is the concentration and θ is the surface coverage.

Values of equilibrium adsorption constant (K_{ads}) obtained determined from the intercept of Equation 4 and related to obtain free energy of adsorption (ΔG_{ads}) in Equation 6:

$$\Delta G_{ads} = -RT \ln (999 K_{ads}) \quad (6)$$

where R is the molar gas constant, T is the room temperature of adsorption and 999 is the molar heat of adsorption of sea water.

Corrosion experimental data achieved was also employed in the Dubinin-Radushkevich Isotherm model (D-RIM). The model explains the mechanism of adsorption of corrosion inhibition and the capability of experimental methods for corrosion. The mathematical model for D-RIM with the maximum surface exposure (θ_{max}) is as follows in equation 7 [3] and the polanyi potential (δ) is given in Equation (8):

$$\text{Lin} \theta = \text{lin} \theta_{max} - a \delta^2 \quad (7)$$

$$\delta = RT \ln \left(1 + \frac{1}{C_{lin}} \right) \quad (8)$$

From the equation, the inhibitor concentration has an absolute temperature (T) and the molar gas constant (R). The constant (a) represents the mean adsorption energy (E) stated in equation (9). This is the transfer energy of 1 mol of adsorbate from infinity (bulk solution) to the adsorbent's surface.

$$E = \frac{1}{\sqrt{2a}} \quad (9)$$

3. Results and discussion

3.1. Weight Loss Measurement

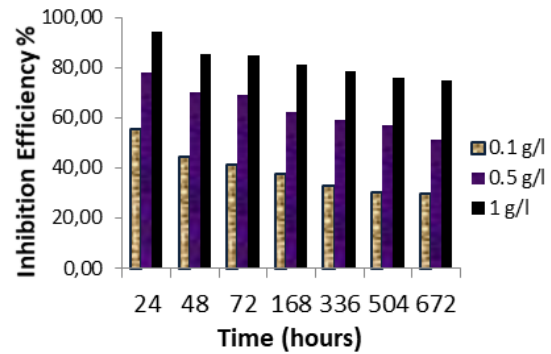
The various corrosion parameters are shown in Table 2 include corrosion rate, surface coverage, and inhibition efficiency that were obtained. On the metal surface, prior to the beginning of the adsorption process of the inhibitor, the corrosion rate was significantly high initially, with little or no inhibitive impact from the extract, regardless of inhibitor concentration. The corrosion rates decreased with an increase in concentrations of the inhibitor (CPE and CSO) and the lowest values of 0.0066 and 0.0054 MPY for CPE and CSO respectively) were obtained by applying the highest concentration (1.0 g/L) of the studied extracts. The values of inhibition efficiency (IE%) and that of surface coverage (θ) for the investigated inhibitors were observed to rise with the increase in inhibitors concentrations, which might be the formation of a passive layer period in the solution. Dimeric film formation on the surface of mild steel right from the period of passive layers formation in the solution resulted in some non-uniformity in values of inhibition efficiency [4].

Table 2. The Corrosion Parameters for Inhibition of AISI 1007 steel in seawater

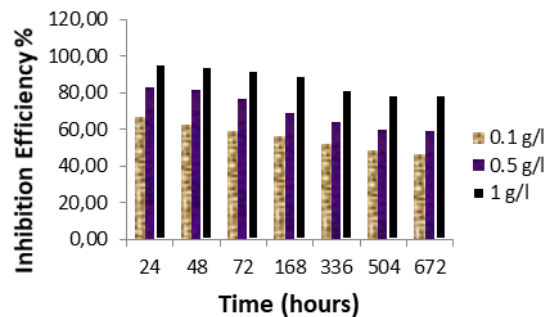
Inhibitors	Concentrations	Corrosion Rate	IE (%)	θ
Blank	-	0.1180	-	-
CPE	0.1	0.0524	55.56	0.5556
	0.5	0.0262	77.78	0.7778
	1.0	0.0066	94.44	0.9444
CSO	0.1	0.0393	66.67	0.6667
	1.0	0.0054	95.44	0.9544

For the studied inhibitors, the IE% was displayed in Figure 2. It can be observed that IE% decreases as immersion time increases. The highest inhibition was recorded at 24 h of immersion as 94.44 % and 95.44 % for CPE and CSO respectively. When

the immersion time was increased, a clear decrease was observed. These results may be due to the instability of the inhibitor layer or due to the biodegradable nature of the plant's extracts after long-time adsorption [8].



(a) CPE Inhibitor



(b) CSO Inhibitor

Fig. 2. Plot of Inhibition Efficiency against Exposure Time for Study Inhibitors

3.2. Electrochemical Measurement

The electrochemical parameters related to Tafel plots like corrosion potential (E_{corr}), corrosion current density (i_{corr}), corrosion potential (E_{corr}), and the corresponding IE% for the corrosion of AISI 1007 steel in seawater solution in the absence and presence of different concentrations (0.1-1.0 g/L) of CPE and CSO at 25 °C are illustrated in Table 3. The results of the inhibited metal specimens in seawater revealed lower i_{corr} values and more positive corrosion potential (E_{corr}) compared to As-received AISI 1007 steel. This suggests that the studied CPE and CSO protect the metal against corrosion through the effective stability of the passive layer.

The value of i_{corr} for 0.1 g/L concentration of studied extracts on the sample was 4.0E-09 A/cm² at 2 hours exposure time which was reduced to 2.47E-09 A/cm² in the case of 0.5 g/L CPE, and 1.14E-09 A/cm² was obtained for 1.0 g/L concentration of CPE. The value of i_{corr} was found to decrease on increasing the concentration of the inhibitors in sea water.

Table 3. Potentiodynamic polarization parameters for corrosion Inhibition of AISI 1007 steel using CPE and CSO in Saline water

Inhibitors	Concentrations	E _{corr} (mV)	I _{corr} (Acm ⁻²)	IE.%	CR (mpy)
Blank	-	-	9.0E-09		4.18E-09
	0.1	0.296	4.0E-09	55.56	1.858E-09
	0.5	0.299	2.47E-09	72.56	1.147E-09
CPE	1.0	0.302	1.14E-09	87.33	5.295E-10
	0.1	0.26	3.42.0E-09	62.00	1.588E-09
CSO	0.5	0.281	1.55E-09	82.78	7.20E-10
	1.0	0.292	0.48E-09	94.67	2.230E-10

The result in sea water of the studied extract at 25 °C revealed that the corrosion current density of AISI 1007 steel decreased and the corrosion inhibition efficiency increased to 87.33% and 94.67% for CPE and CSO respectively. Results also suggest that the addition of 1.0 g/L concentration of studied extract in seawater improves the corrosion inhibitive performance of metal. While the lower i_{corr} values showed the formation of inhibitive strength on the metal surface.

However, the anodic and cathodic parameters of potentiodynamic polarization curves for the tests are shown in Figure 3. The anodic and cathodic current densities as shown in the potentiodynamic polarization curves for the studied inhibitors decreased and this can be explained by the adsorption of organic compounds such as heteroatoms (nitrogen-oxygen, phosphorus, and sulphur) at the AISI 1007 steel surface. The aromatic rings found in organic compounds acted as mixed-type inhibitors. This behavior blocked the reaction sites on the metal surface which is due to the good coverage of the metal surface by inhibitor molecules [1, 3].

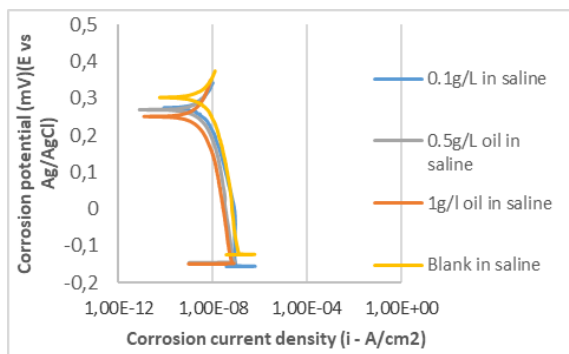


Fig. 3. Corrosion Potential against Corrosion Current Density for CSO Inhibitor

3.3. Adsorption Properties of Corrosion Inhibition Langmuir Adsorption Model

The negative values of free energy of adsorption, ΔG_{ads} , are obtained (Table 4), the negative value of ΔG_{ads} implies a spontaneous adsorption process and the excellent stability of the adsorbed layer on the AISI 1007 steel surface. The value of -ve ΔG_{ads} is greater than 20 kJ/mol that involves an electrostatic interaction between the atoms/ions on the metal surface and the strong adsorbed molecules [1].

Table 4. Langmuir Adsorption Model Parameters

Inhibitors	Methods	K _{ads}	ΔG_{ads}	R ₂
CPE	WL	9.1239	-22.62	0.9955
	PDP	9.7217	-22.77	0.9954
CSO	WL	14.3916	-23.75	0.9978
	PDP	12.6922	-23.44	0.9983

The result of mixed adsorption obtained involves physical and chemical adsorption. Generally, the values of ΔG_{ads} decrement to -20 kJ/mol are consistent with electrostatic interaction between the carbon steel surface and charged molecules of inhibitor (physical adsorption) and those higher than -40 kJ/mol involves transfer or sharing of charge from the molecule inhibitor to a steel surface in order to form a coordinate bond (chemisorption).

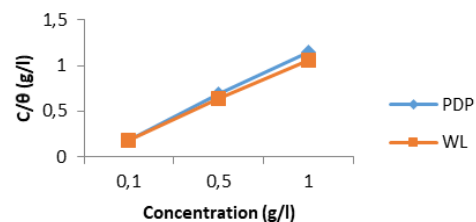


Fig. 4. Plot of Langmuir Adsorption Model

3.4. Dubrimim–Radushkevich Adsorption Model

The type of adsorption was achieved from the information given based on the magnitude of E and once the values are less than 8.0 KJmol⁻¹, it shows physical adsorption [14]. Figure 5 showed the interaction of ln θ for the data obtained from the different methods.

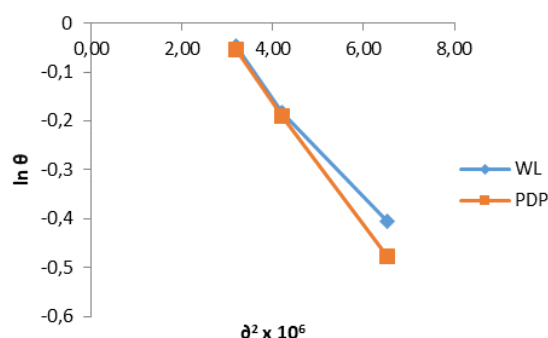


Fig. 5. Plot of D-RIM for Corrosion Inhibition of AISI 1007 Steel in seawater

From the D-RIM, the parameters are stated in Table 5, which reveals the values of energy transfer (E) that indicated the physical adsorption mechanism

Table 5. The D-RIM Adsorption Parameters for Corrosion Inhibition of AISI 1007 Steel in Seawater

Inhibitors	Methods	θ_{max}	a	E	R ²
CPE	Weight loss	15.78	0.1574	6.35	0.97
	PDP	13.91	0.1522	6.56	0.95
CSO	Weight loss	17.47	0.177	5.65	0.96
	PDP	16.78	0.1682	5.94	0.98

Table 6. Phytochemical analysis of Cucumber Peel and Seed oil

Parameter	Cucumber Seed oil	Cucumber Peel
Alkaloids	1.32 (+)	0.89 (+)
Flavonoids	2.86 (+)	2.72 (+)
Tannis	1.16 (+)	0.15 (+)
Saponins	0.09 (+)	0.06 (+)
Terpinoids	0.13 (+)	0.07 (+)
Phenols	0.28 (+)	0.20 (+)
Cardiac glycoside	0.09 (+)	0.08 (+)
Steroids	1.38 (+)	1.32 (+)
Phobatannins	0.18 (+)	0.14 (+)

The presence of a large quantity of flavonoids in cucumber fruit homogenate indicates the ability to

in which the values of maximum surface coverage (θ_{max}) for each of the methods used in this study are in good agreement as similar to the variability of the inhibition efficiency values obtained.

Polyphenols, including phenolic compounds and flavonoids, constitute the main groups of compounds acting as primary antioxidants or free radical scavengers. In the plants, a wide variety of free radicals scavenging molecules that are rich in antioxidant activity such as alkaloids, flavonoids, saponin, tannin, and terpenoids are present [15]. Their antioxidant activity is based on their ability to donate hydrogen atoms to free radicals and their stability as radical intermediates.

It can be observed from the obtained result that both plant extracts have various phytochemical compounds which are presented in Table 6. These extracted compounds chemically bind to AISI 1007 steel by scavenging the free-oxygen radicals that produce a relatively stable radical. The free radicals' metastable chemical entities have a tendency to capture electrons from molecules in their instant local vicinity [16]. This resulted in the creation of a barrier formation on the surface of the specimens in the corrosive attack. It can be observed that both extracts have high flavonoids.

scavenge free radicals as it was reported as the chief source of antioxidant in plants that have been known to play a significant role in free radical scavenging [17].

4. Conclusions

The corrosion inhibition was conducted using weight loss, and electrochemical measurements. CSO displays good inhibition efficiency, while CPE shows a moderate inhibition performance. The inhibition properties revealed that both CPE and CSO mitigate both the anodic and cathodic process (mixed-typed inhibitor) following Langmuir and Dubinin-Radushkevich Isotherm adsorption model. Results showed that the performance of both inhibitors decreased with time. The study showed that both plant extracts contained different phytochemical

compounds which in the adsorption process created a barrier formation on the surface of AISI 1007 steel in the corrosive attack.

Acknowledgments

The authors express their profound gratitude and appreciation to the management of Midwal Engineering Limited, Lekki, Lagos State, Nigeria for their support by allowing us to use their laboratory facilities for some of the tests carried out in this study.

References

- [1]. **Al-Senani G. M.**, *Corrosion inhibition of carbon steel in acidic chloride medium by cucumis sativus (cucumber) peel extract*, International Journal of Electrochemical Science, 11, p. 291-302, 2016.
- [2]. **Shuaib-Babata Y. L., Ibrahim H. K., Ambali I. O., Yahya R. A., Ajao K. S., Aremu N. I., Pelumi A. A.**, *Inhibitive potential of prosopis Africana on corrosion of low carbon steel in 1 M hydrochloric acid medium*. International Journal of Engineering Materials and Manufacture, 4(2), p. 66-76. DOI:10.26776/ijemm.04.02.2019.04, 2019.
- [3]. **Ayawei N., Ebelegi A. N., Wankasi D.**, *Modelling and interpretation of adsorption isotherms*, Hindawi Journal of Chemistry, p. 1-11, DOI:10.1155/2017/3039817, 2017.
- [4]. **Awe I. C., Abdulraman A. S., Ibrahim H. K., Kareem A. G.**, *Inhibitive performance of bitter leaf root extract on mild steel corrosion in sulphuric acid solution*, American Journal of Material Engineering and Technology, 3(2), p. 35-45, 2015.
- [5]. **Odewunmi N., Umoren S., Gasem Z.**, *Utilization of watermelon rind extract as a green corrosion inhibitor for mild steel in acidic media*, Journal of Industrial and Engineering Chemistry, 21, p. 239-247, 2015.
- [6]. **Shuaib-Babata Y. L., Busari Y. O., Yahya R. A., Abdul M.**, *Corrosion inhibition of AISI 1007 steel in hydrochloric acid using cucumis sativus (cucumber) extracts as green inhibitor*, ACTA Technica Corviniensis - Bulletin of Engineering, XI, (4), p. 153-161, 2018.
- [7]. **Idouhli R., Koumya Y., Khadiri M., Aityoub A., Abouelfida A., Benyaich A.**, *Inhibitory effect of Senecio anteuphorbium as green corrosion inhibitor for S300 steel*, International Journal of Industrial Chemistry, 10, p. 133-143, <https://doi.org/10.1007/s40090-019-0179-2>, 2019.
- [8]. **Ali I. H., Idris A. M., Suliman M. H.A.**, *Evaluation of leaf and bark extracts of acacia tortilis as corrosion inhibitors for mild steel in seawater: experimental and studies*, International Journal of Electrochem. Sci., 14, p. 6406-6419, doi: 10.20964/2019.07.10, 2019.
- [9]. ***, *ASTM G4 (1995), Standard guide for conducting corrosion coupon test in field application*, p. 44-53, United States: ASTM International, 100 Barr Harbor Drive, West Conshohocken, PA 19428-2959.
- [10]. ***, *ASTM G1 (1999), Standard Practice for preparing, cleaning, and evaluation corrosion test specimens*, p. 14-21, United States: ASTM International, 100 Barr Harbor Drive, West Conshohocken, PA 19428-2959.
- [11]. ***, *NACE/ ASTM G31-12a, Standard guide for laboratory immersion corrosion testing of metals*, United States: ASTM International, 100 Barr Harbor Drive, West Conshohocken, PA 19428-2959, 2012.
- [12]. **Popov B. V.**, *Corrosion engineering: basics of corrosion measurement*, USA: Elsevier B.V. <http://dx.doi.org/10.1016/B978-0-444-62722-3.00005-7>, 2015.
- [13]. **Fouda A., Elewady G., Shalabi K., Habouba S.**, *Tobacco plant extracts as save corrosion inhibitor for carbon steel in hydrochloric acid solution*, International Journal of Advanced Research, 2, p. 817-832, 2014.
- [14]. **Solomon M. M., Umoren S. A., Udosoro I. I., Udo A. P.**, *Inhibitive and adsorption behavior of carboxymethyl cellulose on mild steel corrosion in sulphuric acid solution*, Corrosion Science, 52, p. 1317-1325, 2010.
- [15]. **Ituen E. B., Udo U. E.**, *Phytochemical profile, adsorptive and inhibitive behavior of costus afer extracts on aluminium corrosion in hydrochloric acid*, Der Chemica Sinica, 3(6), p. 1394-1405, 2012.
- [16]. **Doughari J. H.**, *Phytochemical: Extraction methods, basic structures and mode of action as potential chemotherapeutic agents, phytochemical - A global perspective of their role in nutrition and health*, in Dr Venketeshwer Rao (Ed.), 2012.
- [17]. **Agatemor U. M., Nwodo O. F. C., Anosike C. A.**, *Phytochemical and proximate composition of cucumber (Cucumis sativus) fruit from Nsukka, Nigeria*, African Journal of Biotechnology, 17(38), p. 1215-1219, 2018.